A Deep Transfer Learning Model with Classical Data Augmentation and CGAN to Detect COVID-19 from Chest CT Radiography Digital Images

Article · August 2021

DOI: 10.20944/preprints202004.0252.v1

CITATION
1

READS
17

4 authors, including:

Mohamed Loey
Benha University
42 PUBLICATIONS **675** CITATIONS

SEE PROFILE

Florentin Smarandache
University of New Mexico Gallup
3,461 PUBLICATIONS **31,603** CITATIONS

SEE PROFILE

Nour Eldeen Mahmoud Khalifa
Cairo University
54 PUBLICATIONS **532** CITATIONS

SEE PROFILE

Article

A Deep Transfer Learning Model with Classical Data Augmentation and CGAN to Detect COVID-19 from Chest CT Radiography Digital Images

Mohamed Loey [1*], Florentin Smarandache [2], Nour Eldeen M. Khalifa [3]

[1] Department of Computer Science, Faculty of Computers Artificial Intelligence, Benha University, Benha 13511, Egypt; mloey@fci.bu.edu.eg (M.L.)
[2] Department of Mathematics, University of New Mexico, Gallup Campus, NM 87301, USA; smarand@unm.edu (F.L.)
[3] Department of Information Technology, Faculty of Computers & Artificial Intelligence, Cairo University, Cairo 12613, Egypt; nourmahmoud@cu.edu.eg (N.E.M.K.)

*Correspondence Author: mloey@fci.bu.edu.eg.
Received: - April 2020; Accepted: - April 2020; Published: date

Abstract: The coronavirus disease 2019 (COVID-19) is the fastest transmittable virus caused by severe acute respiratory syndrome coronavirus 2 (SARS-CoV-2). The detection of COVID-19 using artificial intelligence techniques and especially deep learning will help to detect this virus in early stages which will reflect in increasing the opportunities of fast recovery of patients worldwide. This will lead to release the pressure off the healthcare system around the world. In this research, classical data augmentation techniques along with CGAN based on a deep transfer learning model for COVID-19 detection in chest CT scan images will be presented. The limited benchmark datasets for covid-19 especially in chest CT images is the main motivation of this research. The main idea is to collect all the possible images for covid-19 that exists until the very writing of this research and use the classical data augmentations along with CGAN to generate more images to help in the detection of the COVID-19. In this study, five different deep convolutional neural network-based models (AlexNet, VGGNet16, VGGNet19, GoogleNet, and ResNet50) have been selected for the investigation to detect the coronavirus infected patient using chest CT radiographs digital images. The classical data augmentations along with CGAN improve the performance of classification in all selected deep transfer models. The Outcomes show that ResNet50 is the most appropriate classifier to detect the COVID-19 from chest CT dataset using the classical data augmentation and CGAN with testing accuracy of 82.91%.

Keywords: COVID-19, 2019 novel coronavirus, SARS-CoV-2, Deep Transfer Learning, Convolutional Neural Network, Machine Learning, CGAN.

1. Introduction

At the end of February 2003, the Chinese population was infected with a Severe Acute Respiratory Syndrome (SARS) virus causing in Guangdong province in China. SARS was named SARS-CoV and confirmed as a member of the beta coronavirus subgroup [1]. In 2019, Wuhan in China infected by a 2019 novel coronavirus that killed more than hundreds and infected over thousands of humans within few days of the 2019 novel coronavirus epidemic. The World Health Organization (WHO) named The 2019 novel virus as Wuhan coronavirus (2019-nCov) which can cause respiratory disease and severe pneumonia [2]. In 2020, the International Committee on Taxonomy of Viruses (ICTV) announced the Wuhan coronavirus as Severe Acute Respiratory

Preprints (www.preprints.org) | NOT PEER-REVIEWED | Posted: 16 April 2020 doi:10.20944/preprints202004.0252.v1

Syndrome CoronaVirus-2 (SARS-CoV-2) and the disease as Coronavirus disease 2019 (COVID-19) [3–5]. The family of coronaviruses is alpha (α), beta (β), gamma (γ), and delta (δ) coronavirus. 2019-nCov was reported to be a member of the β group of coronaviruses. An epidemic of SARS coronavirus affected 26 countries and outcomes in more than 8000 cases in 2003. An epidemic of SARS-CoV-2 infected more than 1.5 million individuals with death-rate of 4%, across 150 countries, till the date of this writing. The transmission rate of SARS-CoV-2 is higher than SARS coronavirus because of S protein in the RBD region of SARS-CoV-2 may have enhanced its transmission [6].

In 2012, Middle East Respiratory Syndrome (MERS) was reported in Saudi Arabia as an illness caused by a coronavirus. SARS and MERS are Betacoronaviruses (β-CoVs or Beta-CoVs) that transmitted to people from some cats and Arabian camels respectively [7,8]. The sale of wild animals may be the source of coronavirus infection. The discovery of multiple offspring of pangolin coronavirus and their similarity to SARS-CoV-2 suggests that pangolins should be considered as possible hosts of novel coronaviruses. WHO recommendations to reduce the risk of transmission of Coronavirus from animals to humans in wild animal markets [9]. Human-to-human transmission of coronavirus Coronavirus transmission from different cases outside China, namely in Italy [10], US [11], Germany [12], and Vietnam [13], Nepal [14]. On 11 April 2020, SARS-CoV-2 Confirmed more than 1.7 million cases, 400000 recovered cases, and 100000 death cases. Figure 1 shows some statistics about recovered and death cases of COVID-19 [15].

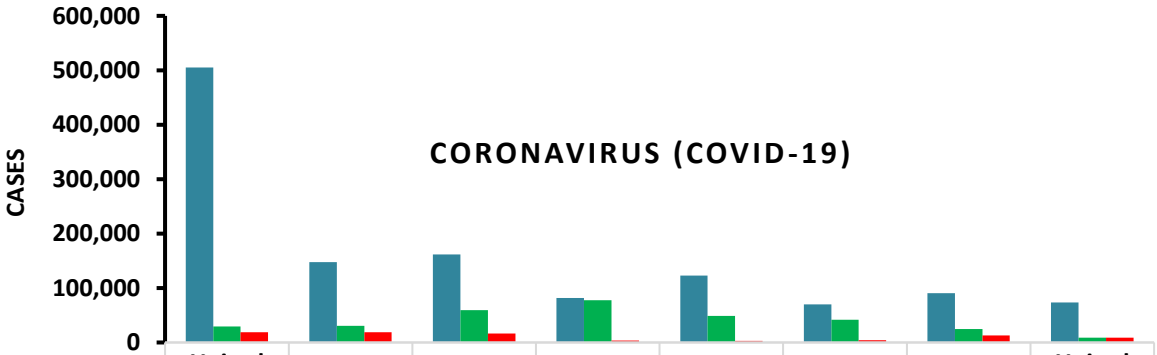

	United States	Italy	Spain	China	Germany	Iran	France	United Kingdom
Confirmed	505,015	147,577	161,852	81,953	122,627	70,029	90,676	73,758
Recovered	29,107	30,445	59,109	77,525	48,692	41,947	24,932	9,000
Deaths	18,771	18,849	16,353	3,339	2,710	4,357	13,197	8,958

Fig. 1. Statistics of COVID-19 in some countries

Deep Transfer Learning (DTL) is a deep learning technique that reused a trained deep learning model that inspired by neurons of the brain [16]. DTL is quickly becoming a critical technique in image/video classification and detection. DTL improves such a medical system to realize higher outcomes, widen illness scope, and implementing applicable real-time medical image [17,18] disease detection systems. In 2012, Krizhevsky and et al. and Ciregan et al. [19,20] showed how Convolutional Neural Networks (CNN/ ConvNet) based on Graphics Processing Unit (GPU) can enhance many image benchmark classification such as MNIST [21], Chinese characters [22], NORB

 doi:10.20944/preprints202004.0252.v1

(jittered, cluttered) [23], traffic signs [24], large-scale ImageNet [25], Arabic digits recognition [26], and Arabic handwritten characters recognition [27]. In the following years, various advances in CNN further decreased the error rate on the image/video classification competition. Many DTL models were introduced as AlexNet [20], VGGNet [28], GoogleNet [29], ResNet [30], Xception [31], DenseNet [32], Inception-V3 [33].

This section conducts the recent scientific papers for applying deep learning in the field of medical chest computerized tomography (CT) classification. Christe et al. [34] introduced a computer-aided detection method based on deep learning was able to detect idiopathic pulmonary fibrosis with similar accuracy to a human reader. The CAD system used for the automatic classification of CT images into 4 radiological diagnostic categories. The model was achieved an F-score (harmonic mean for precision and recall) of 80%. In [35], the authors introduced a novel system for automated classify of Interstitial Lung Abnormality patterns in computed tomography (CT) images. The proposed system was an ensemble of deep convolutional neural networks (DCNNs) that detect more features by incorporating dimensional architectures. The outcome of the ensemble is the sensitivity of 91,41% and specificity of 98,18%.

In this paper, we introduced a deep transfer learning (DTL) models to classify COVID-19 chest CT scan digital images. To input adopting CT images of the chest to the deep convolutional neural network (DCNN), we enriched the medical chest CT images using classical data augmentation and CGAN to generate more CT images. After that, a classifier is used to ensemble the class (COVID/NonCOVID) outputs of the classification outcomes. The proposed DTL model was evaluated on the COVID-19 CT scan images dataset. The novelty of this research is conducted as follows: i) The introduced DTL models have end-to-end structure without classical feature extraction and selection methods. ii) We show that data augmentation and Conditional Generative Adversarial Network (CGAN) is an effective technique to generate CT images. iii) Chest CT images are one of the best tools for the classification of COVID-19. iv) The DTL models have been shown to yield very high accuracy in the limited dataset COVID-19. The rest of the paper is organized as follows. In section 2, discusses the dataset used in our research. In section 3, introduces the proposed models, while section 4 illustrates the achieved outcomes and its discussion. Finally, section 5 provides conclusions and directions for further research.

2. Dataset

The COVID-19 CT scan digital images dataset [36] utilized in this research was created by Zhao et al (https://github.com/UCSD-AI4H/COVID-CT). The authors collected 760 preprints about COVID-19 from bioRxiv1 (https://www.biorxiv.org) and, medRxiv2 (https://www.medrxiv.org) posted from Jan 19th to Mar 25th that report patient cases of COVID-19 CT. The dataset is organized into 3 folders (train, validation, and test) and contains subfolders for each image category (COVID/NonCOVID). There are 742 CT images and 2 categories (COVID/NonCOVID). The number of images for each class is presented in Table 1. Table 1 illustrates that the proposed method to increase the number of COVID-19 CT images using augmentation and CGAN. Figure 2 illustrates samples of CT images used for this research.

Preprints (www.preprints.org) | NOT PEER-REVIEWED | Posted: 16 April 2020 doi:10.20944/preprints202004.0252.v1

Table 1. Number of images for each class in Covid-19 CT dataset

Dataset	Train set		Validation set		Test set	
	COVID	NonCOVID	COVID	NonCOVID	COVID	NonCOVID
COVID19	191	234	60	58	94	105
COVID19 +Aug	2292	2808	720	696	94	105
COVID19 +CGAN	2191	2234	210	208	94	105
COVID19 +Aug+CGAN	4292	4808	870	846	94	105

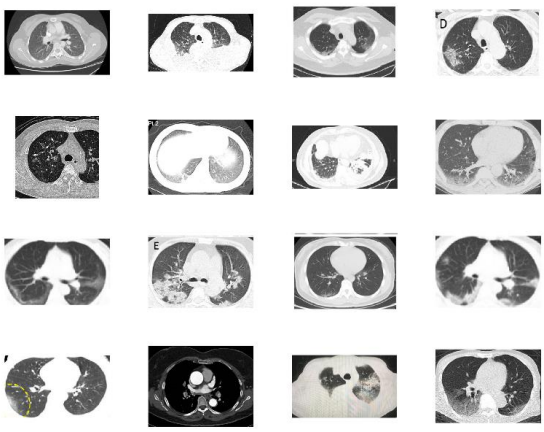

Fig. 2. Samples of the used COVID-19/NonCOVID CT images used in this research

3. Proposed Model

The proposed architecture consists of two main components, the first component is the data augmentation using classical data augmentation techniques along with CGAN, while the second component is the DTL model as shown in figure 3. Mainly, the classical data augmentation and CGAN used in the preprocessing phase while the DTL used in the performance measurement phase.

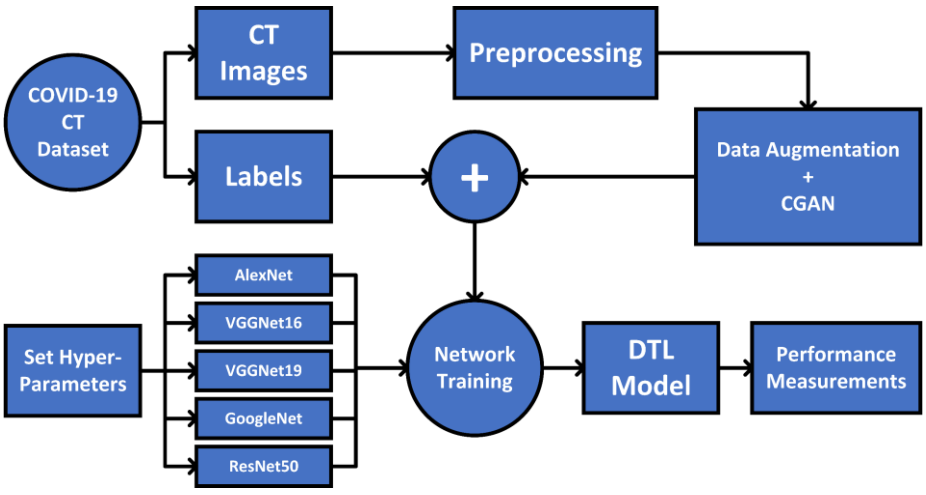

Preprints (www.preprints.org) | NOT PEER-REVIEWED | Posted: 16 April 2020 doi:10.20944/preprints202004.0252.v1

Fig. 3. The proposed architecture of the classical data augmentation along with CGAN and DTL models

Algorithm 1 Proposed Algorithm

Require: COVID-19 CT scan Images (X, Z); where $Z = \{z/z \in \{$ COVID; NonCOVID $\}\}$

Output: The trained DTL model that classifies the COVID-19 CT image $x \in X$

Preprocessing:

- Resize the image to dimension 256 × 256
- Perform data augmentation: Generate COVID-19 CT images
- Perform CGAN: Generate COVID-19 CT images
- Mean normalize each COVID-19 CT scan images

Import a set of DTL models D= { AlexNet, VGGNet16, VGGNet19, GoogleNet, ResNet50}

Replace the last fully connected layer of each model by a layer of (2 × 1) dimension.

foreach $\forall m \in M$ **do**

$\mu = 0.001$

for epochs = 1 to 50 **do**

foreach mini-batch $(X_i; Z_i) \in (\mathrm{X_{train}}; \mathrm{Z_{train}})$ do

Update the parameters of the model $m(\cdot)$

if the validation error is not improving for five epochs **then**

$\mu = \mu \times 0.01$

end

end

end

end

foreach $\forall x \in Z_{test}$ **do**

the output of all models, $m \in M$

end

Algorithm 1 introduces the proposed model in detail below. Let $M =$ {AlexNet, VGGNet16, VGGNet19, GoogleNet, ResNet50} be the set of DTL models. Each DTL is fine-tuned with the COVID-19 CT Images dataset (X, Z); where X the set of N images, each of size, 256 × 256, and Z contain the corresponding labels, $Z = \{z/z \in \{\text{COVID; NonCOVID}\}\}$. The dataset divided to train, validate, and test, training set $(\mathrm{X_{train}}; \mathrm{Z_{train}})$, validate set $(\mathrm{X_{val}}; \mathrm{Z_{val}})$, test set $(\mathrm{X_{test}}; \mathrm{Z_{test}})$. The training data then divided into mini-batches, each of size $n = 32$, such that $(X_i; Z_i) \in (\mathrm{X_{train}}; \mathrm{Z_{train}})$; $i = 1,2, \ldots, \frac{N}{n}$ and iteratively optimizes (fine-tuning) the DCNN model $d \in D$ to reduce the empirical loss as illustrated in equation (1).

$$L(w, X_i) = \frac{1}{n} \sum_{x \in X_i, z \in Z_i} l(m(x, w), z) \qquad (1)$$

where $l(.)$ is the categorical cross − entropy loss penalty function, and $m(x, w)$ is the DCNN model that predicts class z for input x given w is a weight.

Preprints (www.preprints.org) | NOT PEER-REVIEWED | Posted: 16 April 2020 doi:10.20944/preprints202004.0252.v1

3.1 Deep Transfer Learning

Deep Transfer Learning (DTL) is the most successful reuse type of deep convolutional neural network model for image/video classification. A single DTL model contains many different layers of convolution and pooling layer that work on feature extraction from image/video and more complex deep features in deeper layers.

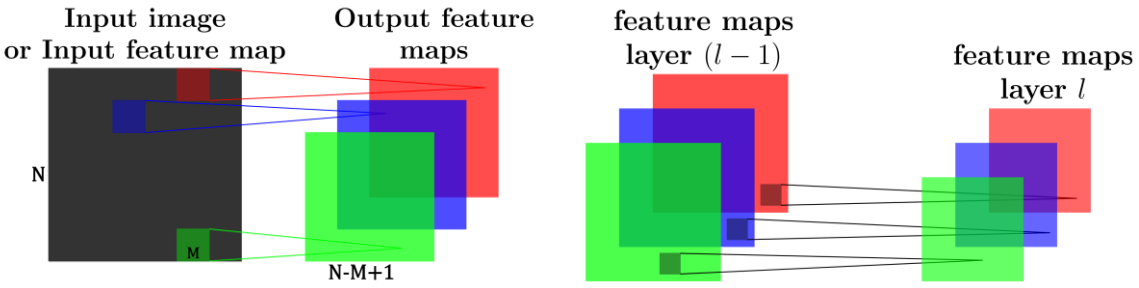

(a) convolutional layer (b) pooling layer

Fig. 4. Illustration of the convolutional and pooling layer which produce feature maps

Let layer l be a convolutional layer. Suppose that we have some $N \times N$ square neuron nodes which are followed by a convolutional layer. If we use an $M \times M$ filter (mask) W then convolutional layer output will be of size $(N - M + 1) \times (N - M + 1)$ which produces k-feature maps that are illustrated in Fig. 4. The convolutional layer acts as a feature extractor that grabs features of the inputs. The convolution layer extract features from the image like edges, lines, and corners. To compute the pre-nonlinearity input to some unit. Then, the input of layer $l - 1$ comprises is computed in equation (2):

$$Z_i^l = B_i^l + \sum_{a=1}^{N}\sum_{b=1}^{N} W_i\, X_{(i+a)(j+b)}^{l-1} \qquad (2)$$

where B_i^l is a bias matrix and W_i is the mask of size $M \times M$. Then, the convolutional layer applies its activation function in equation (3):

$$Net = \sigma(Z_i^l) \qquad (3)$$

where $\sigma(.)$ is called non-linearity, function applied to achieve non-linearity in DTL, which contains many types such as tanh, sigmoid, Rectified Linear Units (ReLU). In our method, we utilize ReLU in equation (4) as the activation function for faster training process:

$$\sigma(u) = \max(0, u) \qquad (4)$$

The loss function is the criterion for the training process. Our loss function in equation (5) is defined as the sum of the cross-entropy loss and the box regression loss:

$$Loss(s, t) = Loss_{cls}(s_{c^*}) + \lambda[p^* > 0] L_{reg}(v, v^*) \qquad (5)$$

where s_{c^*} denotes the predicted score class c^* while v and v^* denote $[v_x, v_y, v_w, v_h]$ of bounding boxes. $\lambda[p^* > 0]$ indicates that we only consider the boxes of non-background (the box is background if $p^* = 0$). This loss function contains two parts for bounding box regression loss $Loss_{reg}$ *and* classification loss $Loss_{cls}$ and, in equation (6-8):

$$Loss_{cls}(s_{c^*}) = -\log(s_{c^*}) \qquad (6)$$

and

Preprints (www.preprints.org) | NOT PEER-REVIEWED | Posted: 16 April 2020 doi:10.20944/preprints202004.0252.v1

$$Loss_{reg}(v, v^*) = \sum_{i\in(x,y,w,h)} R_{L1}(v_i - v_i^*) \quad (7)$$

where:

$$R_{L1}(u) = \begin{cases} 0.5u^2, & if\ |u| < 0 \\ |u| - 0.5, & otherwise \end{cases} \quad (8)$$

3.2 Data Augmentation

The main idea behind this research is to perform a transfer learning with augmented COVID-19 CT images. ,To increase the performance of the proposed transfer learning models, training data amount and validate data amounts is a very important factor. The most popular classical data augmentation method is to perform a combination of the affine image transformations [37]. Different methods for classical data augmentation such as rotation, shifting, flipping, zooming, transformation, add noise were selected to be applied in the original dataset. Figure 5 shows examples of COVID-19 CT augmented images. The achieved performance measurement will be discussed in the experimental results section.

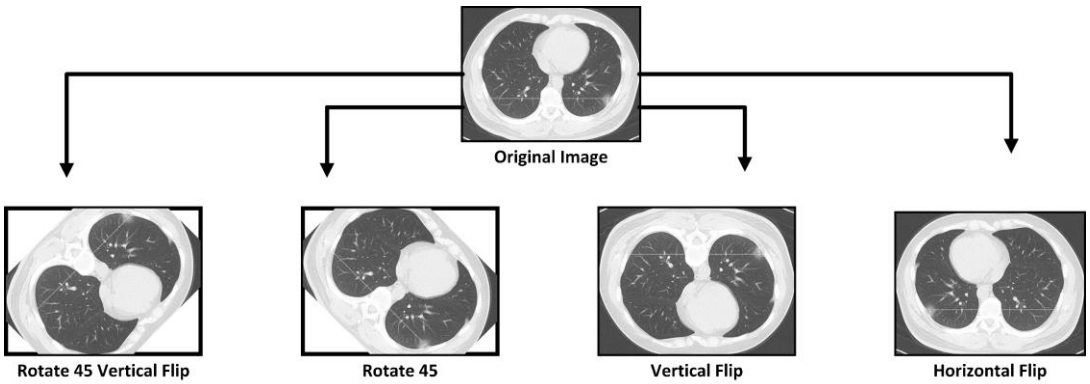

Fig. 5. Perform augmentation methods to increase limited COVID-19 CT scan images

3.3 Conditional Generative Adversarial Network

CGANs consist of two different types of networks (generator Network, discriminator network) with the conditional label as shown in Figure 6. A CGAN is a type of GAN that takes labels in the training process. The generator network in this paper consists of 4 transposed convolutional layers, 3 ReLU layers, 3 batch normalization layers, and Tanh Layer at the end of the model, while the discriminator network consists of 4 convolutional layers, 3 leaky ReLU, and 2 batch normalization layers. All the convolutional and transposed convolutional layers used the same filter size of 5x5 pixels with 20,10, 5 filters for each layer for the generated network but 5,10,20,40 for each layer in the Discriminator network. Figure 7 presents the structure and the sequence of layers of the CGAN network proposed in this research. We trained our CGAN model as shown in the right figure 8, and on the left, some generated CT images.

Preprints (www.preprints.org) | NOT PEER-REVIEWED | Posted: 16 April 2020 doi:10.20944/preprints202004.0252.v1

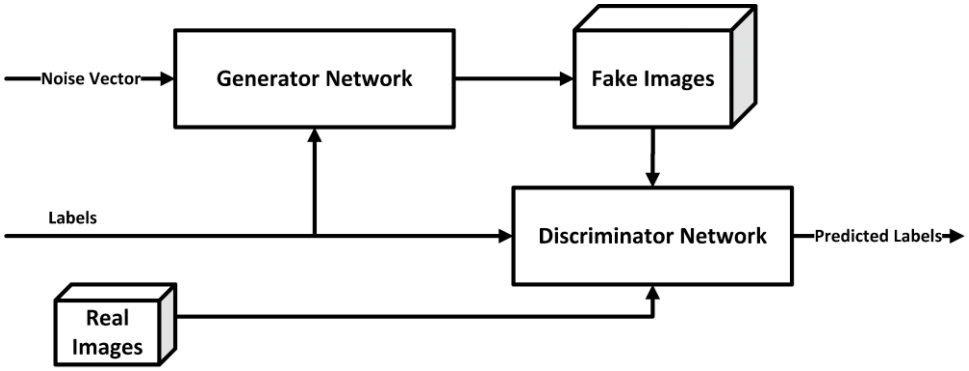

Fig. 6. Conditional Generative Adversarial Network model

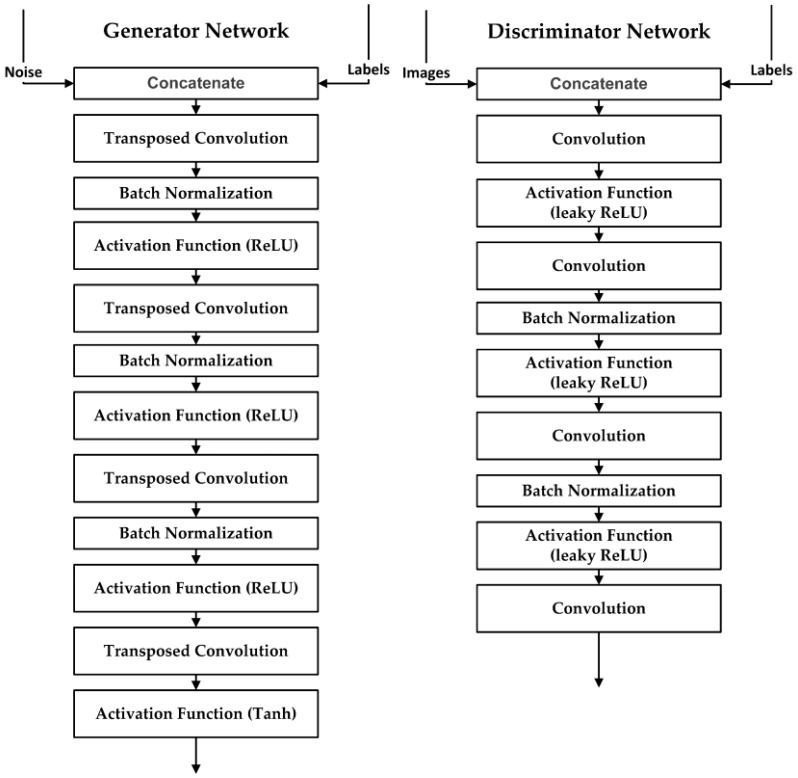

Fig. 7. The structure of the proposed CGAN network

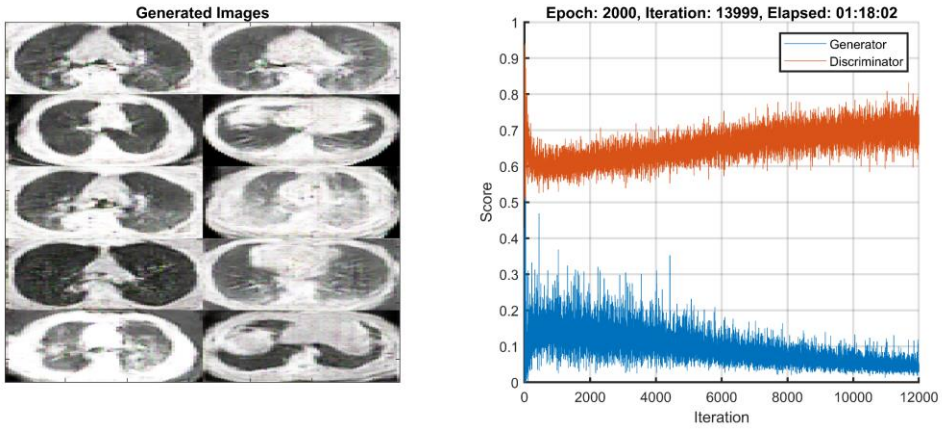

Fig. 8. CGAN training and samples of the generated image

Preprints (www.preprints.org) | NOT PEER-REVIEWED | Posted: 16 April 2020 doi:10.20944/preprints202004.0252.v1

The CGAN network helped in overcoming the overfitting problem caused by the limited number of CT images in the COVID-19 dataset. Figure 7 presents samples of the output of the GAN network for the covid-19 class. Moreover, it increased the dataset images to be 10 times larger than the original one. The dataset number of images reached 4425 images in the train set and 418 in the validation set after using the CGAN network for 2 classes. This will help in achieving better testing accuracy and performance matrices. The achieved performance measurement will be discussed in the experimental results section.

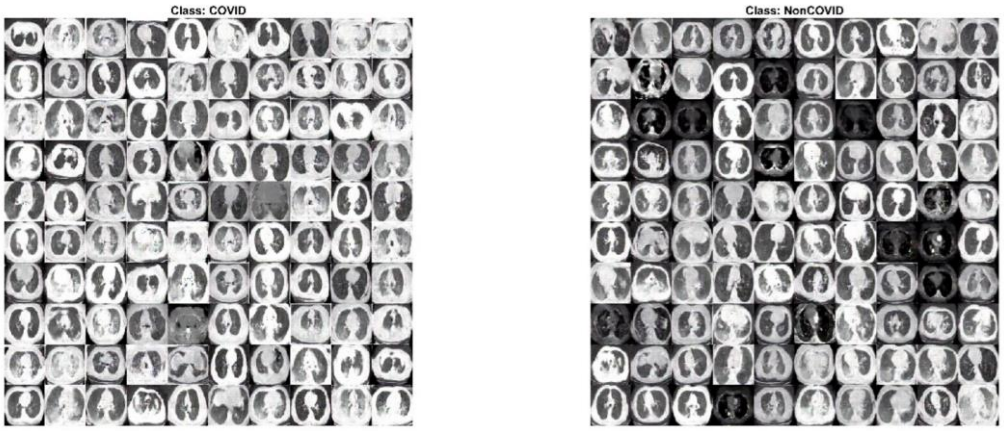

Fig. 9. Samples of COVID-19 CT images generated by the CGAN model.

4. Experimental Results

The proposed model is trained on a high-end Graphics Processing Unit (GPU). The GPU used (NVIDIA RTX 2070) contains 2304 CUDA core and comes with the CUDA Deep Neural Network library (CuDNN) for GPU learning. The deep learning package TensorFlow machine learning and Matlab as back end library. The proposed model has been tested under four different scenarios, the first scenario is to test the DTL models with original COVID-19 CT dataset, the second scenario with data augmentation, the third one with CGAN, and the last one combines all three scenarios. All the test experiment scenarios included the two classes (COVID/NonCOVID). Every scenario consists of the validation phase and the testing phase as shown in Table 2.

Table 2. Configuration of DTL models

Model	Layers	Batch size	Momentum	Epoch	Learning Rate	Optimizer
AlexNet	8	32	0.9	50	0.001	Adam
VGGNet16	16					
VGGNet19	19					
GoogleNet	22					
ResNet50	50					

Table 2 shows the five DTL models with initial learning rate (μ) equal to 0.001 and the number of epochs equal to 50. Also, the mini-batch size is set to 32 and early-stopping to be 5 epochs if the accuracy didn't improve. In terms of optimizer technique, Adam [38] is chosen as our optimizer

Preprints (www.preprints.org) | NOT PEER-REVIEWED | Posted: 16 April 2020 doi:10.20944/preprints202004.0252.v1

technique, which updates weights parameters. This optimizer technique is a combination of Root Mean Square Propagation (RMSprop) and Stochastic Gradient Descent (SGD) with momentum. To avoid deep learning network overfitting problems, we utilize this problem by using the dropout method [39] as well as the early-stopping technique [40] to select the most appropriate training iteration.

4.1 Verification and Testing Accuracy Measurement

Testing accuracy is one of the estimations which demonstrates the performance measurement of any DTL models. The confusion matrix also is one of the performance measurements which give more insights into the achieved testing accuracy. The first DTL model will be investigated is AlexNet along with four scenarios as shown in Figure 10. Figure 10 shows that the highest testing accuracy is 76.4% when the COVID-19 CT dataset is augmented with data augmentation along with CGAN. The Second DTL model will be investigated with VGGNet16. Figure 10 shows that the highest testing accuracy is 78.9% when the COVID-19 CT dataset is augmented with classical data augmentation along with CGAN. The Third DTL model will be investigated with VGGNet19. Figure 10 shows that the highest testing accuracy is 76.9% when the COVID-19 CT dataset is not augmented. The Fourth DTL model will be investigated with GoogleNet. Figure 10 shows that the highest testing accuracy is 77.4% when the COVID-19 CT dataset is augmented with the classical data augmentation along with CGAN.

The Final DTL model will be investigated with ResNet50. Figure 10 shows that the highest testing accuracy is 82.9% when the COVID-19 CT dataset is augmented with classical data augmentation as shown in Figure 11. Table 3 summarizes the testing accuracy for the different deep transfer learning models for 2 classes with the four scenarios. Table 3 illustrates according to testing accuracy, the Resnet50 achieved the highest accuracy with 82.9%, this is due to the large number of parameters in the Resnet50 architecture which contains millions of parameters which are not larger than VGGNet and GoogleNet but the VGGNet and GoogleNet only include 16, and 22 layers while the Resnet50 includes 50 layers.

Table 3. DTL testing accuracy for the different four scenarios

Dataset	AlexNet	VGGNet16	VGGNet19	GoogleNet	ResNet50
COVID-19	67.34%	72.36%	76.88%	75.38%	76.38%
COVID-19 with augmentation	75.38%	77.89%	69.35%	76.88%	**82.91%**
COVID-19 with GAN	68.34%	70.85%	73.37%	75.88%	77.39%
COVID-19 with aug and GAN	76.38%	78.89%	73.87%	77.39%	81.41%

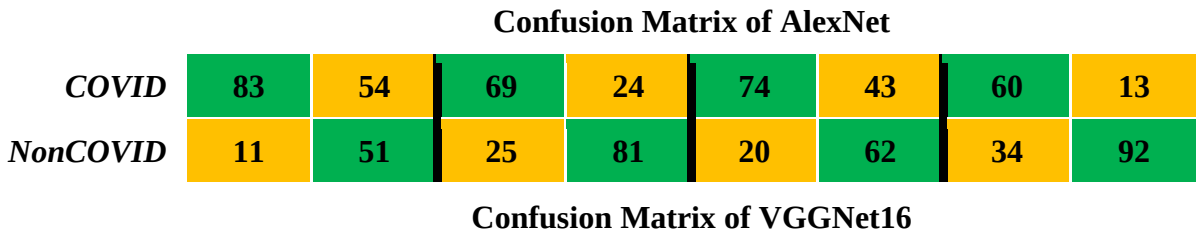

Preprints (www.preprints.org) | NOT PEER-REVIEWED | Posted: 16 April 2020 doi:10.20944/preprints202004.0252.v1

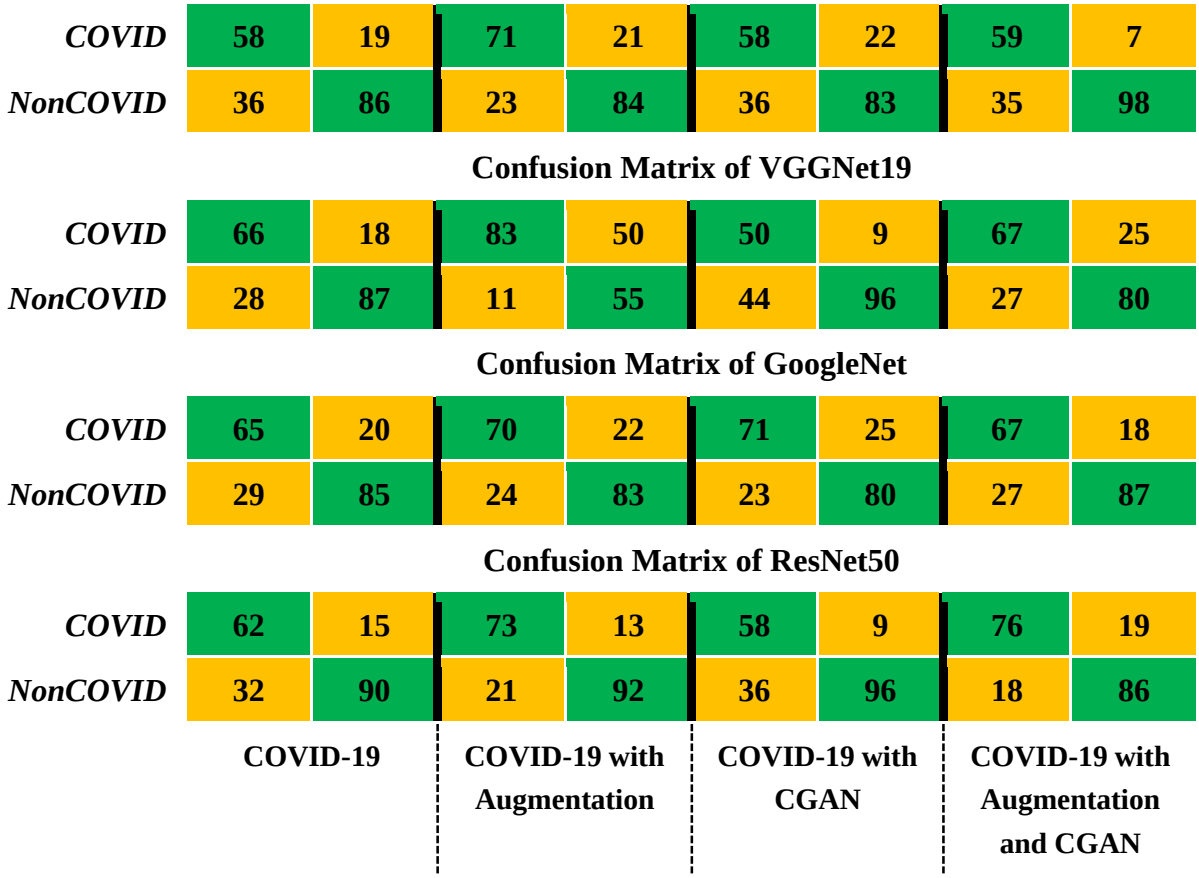

Fig. 10. DTL Confusion matrices for two classes with different scenarios

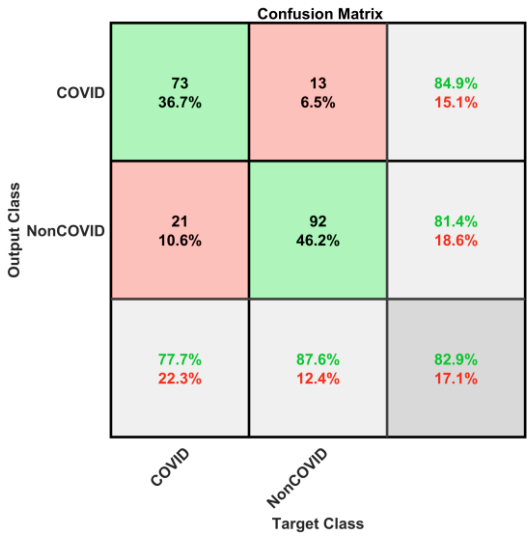

Fig. 11. Confusion matrix of highest accuracy for ResNet50 in COVID-19 with classical data augmentation

4.2 Performance Evaluation and Discussion

To quantitatively evaluate the performance measurement of the proposed model, more performance matrices are needed to be investigated through this paper. The most common performance measures in the field of deep learning are Sensitivity, Specificity, Precision, Accuracy and F1 Score [41] and they are presented from equation (9) to equation (13).

Preprints (www.preprints.org) | NOT PEER-REVIEWED | Posted: 16 April 2020 doi:10.20944/preprints202004.0252.v1

$$\text{Accuracy} = \frac{\text{TP+TN}}{(\text{TP+FP})+(TN+FN)} \quad (9)$$

where TP (True Positives) is the count of correctly labeled instances of the class under observation, FP (False Positives) is the count of miss-classified labeled of rest of the classes, TN (True Negatives) is the count of correctly labeled instances of rest of the classes, and FN (False Negatives) is the count of miss-classified labeled of the class under observation.

$$\text{Sensitivity} = \frac{\text{TP}}{(\text{TP+FN})} \quad (10)$$

$$\text{Specificity} = \frac{\text{TP}}{(\text{FP+TN})} \quad (11)$$

$$\text{Precision} = \frac{\text{TP}}{(\text{TP+FP})} \quad (12)$$

$$\text{F1 Score} = \frac{2\text{TP}}{(2\text{TP+FP+FN})} \quad (13)$$

Figure 12 presents the performance metrics for different scenarios with DTL models for the COVID-19 CT dataset. The highest sensitivity of 88.3% (Table 4) is achieved by scenario-1 and scenario-2 (COVID-19 only and with augmentation) based on AlexNet and VGGNet19 that refers to the test's ability to correctly classify COVID-19 CT patients who do have the condition. In the example of a CT scan medical test used to classify and detect a COVID-19 disease, the detection rate (sensitivity) of the test is the proportion of people who test positive for the COVID-19 malady among those who have the COVID-19 malady. A negative result in a test with a high detection rate is useful for getting rid of the COVID-19 CT malady.

A test with high specificity would be able to determine the human that does not have the COVID-19 as shown in Table 5. Sensitivity and specificity can be summarized by a single quantity called the balanced accuracy as shown in Table 6, which is defined as the mean of both measures in equation (14):

$$\text{Balanced accuracy} = \frac{\text{Sensitivity+Specificity}}{2} \quad (14)$$

The balanced accuracy is in the range [0,1] where a value of 0 and 1 indicate the worst and the best classifier, respectively.

Preprints (www.preprints.org) | NOT PEER-REVIEWED | Posted: 16 April 2020 doi:10.20944/preprints202004.0252.v1

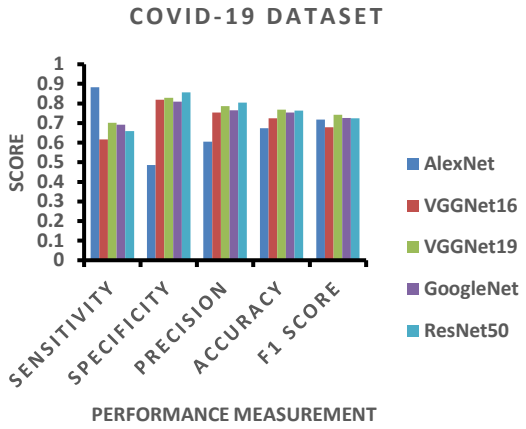

(a) COVID-19

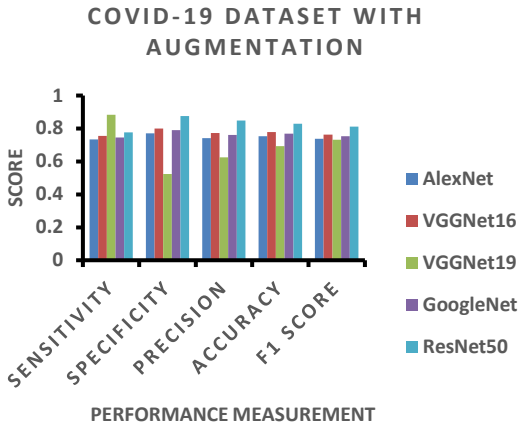

(b) COVID-19 with Augmentation

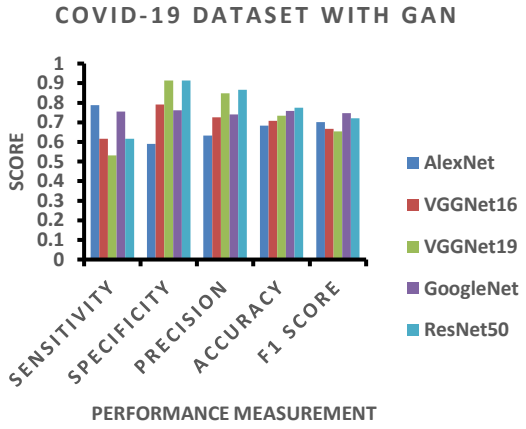

(c) COVID-19 with CGAN

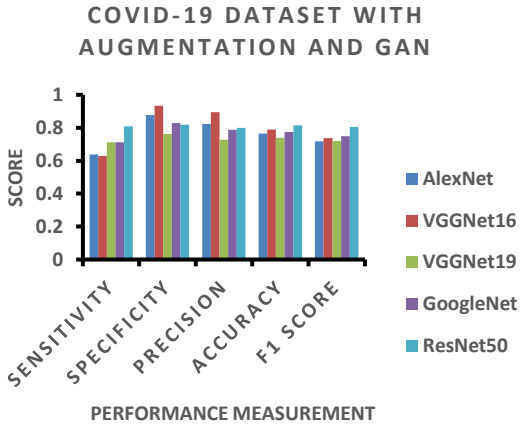

(d) COVID-19 with Augmentation and CGAN

Fig. 12. Performance measurements for COVID-19 CT in four scenarios

Table 4. Testing Sensitivity for the different 4 scenarios

Dataset	AlexNet	VGGNet16	VGGNet19	GoogleNet	ResNet50
COVID-19	**88.30%**	61.70%	70.21%	69.15%	65.96%
COVID-19 with augmentation	73.40%	75.53%	**88.30%**	74.47%	77.66%
COVID-19 with CGAN	78.72%	61.70%	53.19%	75.53%	61.70%
COVID-19 with aug and CGAN	63.83%	62.77%	71.28%	71.28%	80.85%

Table 5. Testing Specificity for the different 4 scenarios

Dataset	AlexNet	VGGNet16	VGGNet19	GoogleNet	ResNet50
COVID-19	48.57%	81.90%	82.86%	80.95%	85.71%
COVID-19 with augmentation	77.14%	80.00%	52.38%	79.05%	87.62%
COVID-19 with CGAN	59.05%	79.05%	91.43%	76.19%	91.43%
COVID-19 with aug and CGAN	87.62%	**93.33%**	76.19%	82.86%	81.90%

Table 6. Testing Balanced accuracy for the different 4 scenarios

Dataset	AlexNet	VGGNet16	VGGNet19	GoogleNet	ResNet50
COVID-19	68.44%	71.80%	**76.54%**	75.05%	75.84%
COVID-19 with augmentation	75.27%	77.77%	70.34%	76.76%	**82.64%**
COVID-19 with CGAN	68.89%	70.38%	72.31%	75.86%	**76.57%**
COVID-19 with aug and CGAN	75.73%	78.05%	73.74%	77.07%	**81.38%**

As shown in Table 6, the balanced accuracy for different scenarios. The table also indicates that ResNet50 is the best classifier to detect the COVID-19 in CT dataset with classical data augmentation along with CGAN. The classical data augmentation along with CGAN improves the performance of classification in all deep transfer models (AlexNet, VGGNet16, VGGNet19, GoogleNet, ResNet50). The other bottleneck is the limited size of the COVID-19 CT database. Predictably the performance of deep transfer models can be further improved if more data are collected in the future. Although, we have achieved promising accuracy rates, however, the proposed model in this study needs to be tested on larger scale datasets that include different COVID-19 CT images to increase the testing accuracy and extend it in other medical applications. As future work, we plan to classify COVID-19 using a neutrosophic approach [42] and deep learning.

5. Conclusion and future works

In 2019, World infected by a 2019 novel coronavirus that killed more than thousands and infected over millions of humans within few months of the 2019 novel coronavirus epidemic. In this paper, classical data augmentations along with CGAN with deep transfer learning for COVID-19 detection in limited chest CT scan images is presented. The number of COVID-19 CT images of the collected dataset was 742 images for two types of labels. The classical data augmentation and CGAN help to increase the CT dataset and overcoming the overfitting problem. Moreover, five deep transfer learning models (AlexNet, VGGNet16, VGGNet19, GoogleNet, ResNet50) were selected in this paper for investigation. Using a combination of classical data augmentation and CGAN with deep transfer learning improve testing accuracy, and performance measurements such as sensitivity, specificity, precision, accuracy, and F1 score. The results show that ResNet50 with classical data augmentation along with CGAN is the best classifier to detect the COVID-19 from chest CT dataset. As future work, we plan to approach the COVID-19 study from a neutrosophic environment with deep learning.

References

1. Chang, L.; Yan, Y.; Wang, L. Coronavirus Disease 2019: Coronaviruses and Blood Safety. *Transfusion Medicine Reviews* **2020**, doi:https://doi.org/10.1016/j.tmrv.2020.02.003.
2. Singhal, T. A Review of Coronavirus Disease-2019 (COVID-19). *The Indian Journal of Pediatrics* **2020**, *87*, 281–286, doi:10.1007/s12098-020-03263-6.
3. Lai, C.-C.; Shih, T.-P.; Ko, W.-C.; Tang, H.-J.; Hsueh, P.-R. Severe acute respiratory syndrome coronavirus 2 (SARS-CoV-2) and coronavirus disease-2019 (COVID-19):

The epidemic and the challenges. *International Journal of Antimicrobial Agents* **2020**, *55*, 105924, doi:https://doi.org/10.1016/j.ijantimicag.2020.105924.

4. Li, J.; Li, J. (Justin); Xie, X.; Cai, X.; Huang, J.; Tian, X.; Zhu, H. Game consumption and the 2019 novel coronavirus. *The Lancet Infectious Diseases* **2020**, *20*, 275–276, doi:10.1016/S1473-3099(20)30063-3.
5. Sharfstein, J.M.; Becker, S.J.; Mello, M.M. Diagnostic Testing for the Novel Coronavirus. *JAMA* **2020**, doi:10.1001/jama.2020.3864.
6. Shereen, M.A.; Khan, S.; Kazmi, A.; Bashir, N.; Siddique, R. COVID-19 infection: Origin, transmission, and characteristics of human coronaviruses. *Journal of Advanced Research* **2020**, *24*, 91–98, doi:https://doi.org/10.1016/j.jare.2020.03.005.
7. Rabi, F.A.; Al Zoubi, M.S.; Kasasbeh, G.A.; Salameh, D.M.; Al-Nasser, A.D. SARS-CoV-2 and Coronavirus Disease 2019: What We Know So Far. *Pathogens* **2020**, *9*, 231, doi:10.3390/pathogens9030231.
8. York, A. Novel coronavirus takes flight from bats? *Nature Reviews Microbiology* **2020**, *18*, 191, doi:10.1038/s41579-020-0336-9.
9. Lam, T.T.-Y.; Shum, M.H.-H.; Zhu, H.-C.; Tong, Y.-G.; Ni, X.-B.; Liao, Y.-S.; Wei, W.; Cheung, W.Y.-M.; Li, W.-J.; Li, L.-F.; et al. Identifying SARS-CoV-2 related coronaviruses in Malayan pangolins. *Nature* **2020**, doi:10.1038/s41586-020-2169-0.
10. Giovanetti, M.; Benvenuto, D.; Angeletti, S.; Ciccozzi, M. The first two cases of 2019-nCoV in Italy: Where they come from? *Journal of Medical Virology* **2020**, *92*, 518–521, doi:10.1002/jmv.25699.
11. Holshue, M.L.; DeBolt, C.; Lindquist, S.; Lofy, K.H.; Wiesman, J.; Bruce, H.; Spitters, C.; Ericson, K.; Wilkerson, S.; Tural, A.; et al. First Case of 2019 Novel Coronavirus in the United States. *New England Journal of Medicine* **2020**, *382*, 929–936, doi:10.1056/NEJMoa2001191.
12. Rothe, C.; Schunk, M.; Sothmann, P.; Bretzel, G.; Froeschl, G.; Wallrauch, C.; Zimmer, T.; Thiel, V.; Janke, C.; Guggemos, W.; et al. Transmission of 2019-nCoV Infection from an Asymptomatic Contact in Germany. *New England Journal of Medicine* **2020**, *382*, 970–971, doi:10.1056/NEJMc2001468.
13. Phan, L.T.; Nguyen, T. V; Luong, Q.C.; Nguyen, T. V; Nguyen, H.T.; Le, H.Q.; Nguyen, T.T.; Cao, T.M.; Pham, Q.D. Importation and Human-to-Human Transmission of a Novel Coronavirus in Vietnam. *New England Journal of Medicine* **2020**, *382*, 872–874, doi:10.1056/NEJMc2001272.
14. Bastola, A.; Sah, R.; Rodriguez-Morales, A.J.; Lal, B.K.; Jha, R.; Ojha, H.C.; Shrestha, B.; Chu, D.K.W.; Poon, L.L.M.; Costello, A.; et al. The first 2019 novel coronavirus case in Nepal. *The Lancet Infectious Diseases* **2020**, *20*, 279–280, doi:10.1016/S1473-3099(20)30067-0.
15. Coronavirus (COVID-19) map Available online: https://www.google.com/covid19-map/ (accessed on Apr 11, 2020).
16. Rong, D.; Xie, L.; Ying, Y. Computer vision detection of foreign objects in walnuts using deep learning. *Computers and Electronics in Agriculture* **2019**, *162*, 1001–1010, doi:https://doi.org/10.1016/j.compag.2019.05.019.

17. Lundervold, A.S.; Lundervold, A. An overview of deep learning in medical imaging focusing on MRI. *Zeitschrift für Medizinische Physik* **2019**, *29*, 102–127, doi:https://doi.org/10.1016/j.zemedi.2018.11.002.
18. Maier, A.; Syben, C.; Lasser, T.; Riess, C. A gentle introduction to deep learning in medical image processing. *Zeitschrift für Medizinische Physik* **2019**, *29*, 86–101, doi:https://doi.org/10.1016/j.zemedi.2018.12.003.
19. Ciregan, D.; Meier, U.; Schmidhuber, J. Multi-column deep neural networks for image classification. In Proceedings of the 2012 IEEE Conference on Computer Vision and Pattern Recognition; 2012; pp. 3642–3649.
20. Krizhevsky Ilya and Hinton Alex and Sutskever, G.E. Imagenet classification with deep convolutional neural networks. *Advances in neural information processing systems* **2012**, 1097–1105.
21. Lecun, Y.; Bottou, L.; Bengio, Y.; Haffner, P. Gradient-based learning applied to document recognition. *Proceedings of the IEEE* **1998**, *86*, 2278–2324, doi:10.1109/5.726791.
22. Yin, F.; Wang, Q.; Zhang, X.; Liu, C. ICDAR 2013 Chinese Handwriting Recognition Competition. In Proceedings of the 2013 12th International Conference on Document Analysis and Recognition; 2013; pp. 1464–1470.
23. LeCun, Y.; Huang, F.J.; Bottou, L. Learning methods for generic object recognition with invariance to pose and lighting. In Proceedings of the Proceedings of the 2004 IEEE Computer Society Conference on Computer Vision and Pattern Recognition, 2004. CVPR 2004.; 2004; Vol. 2, pp. II-104 Vol.2.
24. Stallkamp, J.; Schlipsing, M.; Salmen, J.; Igel, C. The German Traffic Sign Recognition Benchmark: A multi-class classification competition. In Proceedings of the The 2011 International Joint Conference on Neural Networks; 2011; pp. 1453–1460.
25. Deng, J.; Dong, W.; Socher, R.; Li, L.; Kai, L.; Li, F.-F. ImageNet: A large-scale hierarchical image database. In Proceedings of the 2009 IEEE Conference on Computer Vision and Pattern Recognition; 2009; pp. 248–255.
26. El-Sawy, A.; EL-Bakry, H.; Loey, M. CNN for Handwritten Arabic Digits Recognition Based on LeNet-5 BT - Proceedings of the International Conference on Advanced Intelligent Systems and Informatics 2016.; Hassanien, A.E., Shaalan, K., Gaber, T., Azar, A.T., Tolba, M.F., Eds.; Springer International Publishing: Cham, 2017; pp. 566–575.
27. El-Sawy, A.; Loey, M.; EL-Bakry, H. Arabic Handwritten Characters Recognition Using Convolutional Neural Network. *WSEAS Transactions on Computer Research* **2017**, *5*.
28. Liu, S.; Deng, W. Very deep convolutional neural network based image classification using small training sample size. In Proceedings of the 2015 3rd IAPR Asian Conference on Pattern Recognition (ACPR); 2015; pp. 730–734.
29. Szegedy, C.; Wei, L.; Yangqing, J.; Sermanet, P.; Reed, S.; Anguelov, D.; Erhan, D.; Vanhoucke, V.; Rabinovich, A. Going deeper with convolutions. In Proceedings of the 2015 IEEE Conference on Computer Vision and Pattern Recognition (CVPR); 2015; pp. 1–9.

30. He, K.; Zhang, X.; Ren, S.; Sun, J. Deep Residual Learning for Image Recognition. In Proceedings of the 2016 IEEE Conference on Computer Vision and Pattern Recognition (CVPR); 2016; pp. 770–778.
31. Chollet, F. Xception: Deep Learning with Depthwise Separable Convolutions. In Proceedings of the 2017 IEEE Conference on Computer Vision and Pattern Recognition (CVPR); 2017; pp. 1800–1807.
32. Huang, G.; Liu, Z.; Maaten, L. v. d.; Weinberger, K.Q. Densely Connected Convolutional Networks. In Proceedings of the 2017 IEEE Conference on Computer Vision and Pattern Recognition (CVPR); 2017; pp. 2261–2269.
33. Szegedy, C.; Vanhoucke, V.; Ioffe, S.; Shlens, J.; Wojna, Z. Rethinking the inception architecture for computer vision. In Proceedings of the Proceedings of the IEEE conference on computer vision and pattern recognition; 2016; pp. 2818–2826.
34. Christe, A.; Peters, A.A.; Drakopoulos, D.; Heverhagen, J.T.; Geiser, T.; Stathopoulou, T.; Christodoulidis, S.; Anthimopoulos, M.; Mougiakakou, S.G.; Ebner, L. Computer-Aided Diagnosis of Pulmonary Fibrosis Using Deep Learning and CT Images. *Investigative Radiology* **2019**, *54*, 627–632, doi:10.1097/RLI.0000000000000574.
35. Bermejo-Peláez, D.; Ash, S.Y.; Washko, G.R.; San José Estépar, R.; Ledesma-Carbayo, M.J. Classification of Interstitial Lung Abnormality Patterns with an Ensemble of Deep Convolutional Neural Networks. *Scientific Reports* **2020**, *10*, 1–15, doi:10.1038/s41598-019-56989-5.
36. Zhao, J.; Zhang, Y.; He, X.; Xie, P. COVID-CT-Dataset: A CT Scan Dataset about COVID-19. *arXiv:2003.13865 [cs, eess, stat]* **2020**.
37. Mikołajczyk, A.; Grochowski, M. Data augmentation for improving deep learning in image classification problem. In Proceedings of the 2018 International Interdisciplinary PhD Workshop (IIPhDW); 2018; pp. 117–122.
38. Kingma, D.P. Adam: A Method for Stochastic Optimization. **2015**.
39. Srivastava, N.; Hinton, G.; Krizhevsky, A.; Sutskever, I.; Salakhutdinov, R. Dropout: A Simple Way to Prevent Neural Networks from Overfitting. *Journal of Machine Learning Research* **2014**, *15*, 1929–1958.
40. Caruana, R.; Lawrence, S.; Giles, L. Overfitting in Neural Nets: Backpropagation, Conjugate Gradient, and Early Stopping. In Proceedings of the Proceedings of the 13th International Conference on Neural Information Processing Systems; MIT Press: Cambridge, MA, USA, 2000; pp. 381–387.
41. Goutte, C.; Gaussier, E. A Probabilistic Interpretation of Precision, Recall and F-Score, with Implication for Evaluation. In; 2010.
42. Smarandache, F. Neutrosophic Set is a Generalization of Intuitionistic Fuzzy Set, Inconsistent Intuitionistic Fuzzy Set (Picture Fuzzy Set, Ternary Fuzzy Set), Pythagorean Fuzzy Set, q-Rung Orthopair Fuzzy Set, Spherical Fuzzy Set, etc. *arXiv:1911.07333 [math]* **2019**.